Analysis of ion temperature gradient modes in high β plasmas with sheared slab configuration model

Zhe Gao[a)]
Department of Engineering Physics, Tsinghua University, Beijing 100084, People's Republic of China

J. Q. Dong
Southwestern Institute of Physics, Chengdu 610041, People's Republic of China

G. J. Liu and C. T. Ying
Department of Engineering Physics, Tsinghua University, Beijing 100084, People's Republic of China

(Received 16 October 2001; accepted 19 November 2001)

A set of integral equations is developed to study drift instabilities in any β (plasma pressure/magnetic pressure) plasmas with the sheared slab magnetic configuration model. Both components of the perturbed vector potential, $\tilde{A}_{\parallel}$ and $\tilde{A}_{\perp}$, are considered in the equations, as well as the perturbation of the electrostatic potential $\tilde{\phi}$. The magnetic gradient drift effects are taken into account. The ion temperature gradient modes are analyzed and found to be unstable in the high β regime. The stability of the high β modes is very sensitive to the mode frequency. The lower frequency modes are more difficult to be stabilized since the β effects cannot effectively change the frequency and then the particle-wave interaction in the lower frequency regime. The magnetic shear is shown to have strong stabilizing effects on the high β modes. [DOI: 10.1063/1.1436125]

I. INTRODUCTION

The ion temperature gradient mode (ITG, η_i mode) has been considered as a candidate to cause the anomalous ion transport in tokamak plasmas.[1–3] Numerous theoretical studies have been done. The analyses[1,4–7] of electrostatic modes have established the basic stability properties of very low β ($\beta=8\pi P/B^2 \ll \sqrt{m_e/m_i}$) plasmas with ion temperature gradients. Later, the behaviors of the ITG modes in finite β plasmas attracted more attention.[8–16] The common conclusion is that a finite β can effectively stabilize the ITG mode. For example, the fundamental slab mode can be completely stabilized with $\beta \leqslant 3\%$ (Ref. 8) at the Linsker's parameters.[4] It seems that the ITG modes are no longer important in higher β devices, such as spherical tokamaks.[17] However, this previous conclusion cannot be arbitrarily applied in high β cases because it is based on the low β assumption. Most previous electromagnetic ITG mode studies[8,11–15] only considered the electrostatic potential $\tilde{\phi}$ and the parallel vector potential $\tilde{A}_{\parallel}$ while neglecting the perpendicular vector potential $\tilde{A}_{\perp}$, which is a good approximation only for low β plasmas. Moreover, the magnetic gradient is needed to maintain pressure equilibrium for high β plasmas even in a slab, even though many previous electromagnetic studies in a slab[8,15] did not consider it. So it is of interest to ask whether the instabilities persist in high β slab plasmas.

Local studies ($k_{\parallel}=$const) of the slab modes[9,16] have shown that the full β effects, especially the magnetic gradient effect, are very important in the high β regime. However, the dispersion relation of the local mode is a simple algebraic equation. The mode structure is not considered and the parallel wave number is rather arbitrary in local studies. Therefore, a nonlocal approach is needed to properly analyze the mode stability properties. If the radial wavelength of the unstable mode is long ($|\rho_i \partial/\partial x| \ll 1$), a differential form of the dispersion equation governs the eigenfrequency and the mode structure. However, as noted by Reynders,[15] the integral form is more general and is valid in the $|\rho_i \partial/\partial x| \sim O(1)$ regime so it is suitable for analyzing modes with fine-scale structures.

An earlier integral eigenmode equation was derived and numerically solved by Tang *et al.*[18] for an artificially small mass ratio $m_i/m_e=100$. Later, Linsker[4] solved the problem for realistic mass ratios. The first linear integral eigenmode study of the finite β modified ITG mode in a sheared slab was performed in the low β limit by Dong *et al.*,[8] where the eigenmode equation was derived from the linearized Vlasov–Maxwell system of self-consistent equations. Reynders[15] derived the same equation directly from the electromagnetic gyrokinetic equation. The present work derives and numerically solves the linear integral eigenmode equation of the ITG instabilities for arbitrary β values in a sheared slab with the magnetic gradient included. This work can be considered as an extension of Dong *et al.*[8] to include the effects of $\tilde{A}_{\perp}$ and magnetic gradient drift, and, on the other hand, as a consequence to our previous local work.[16]

The organization of this paper is as follows. Section II presents the integral eigenmode equations. The numerical results and some analyses are described in Sec. III. Section IV is devoted to conclusions and discussion.

[a)]Electronic mail: gaozhe97@mails.tsinghua.edu.cn

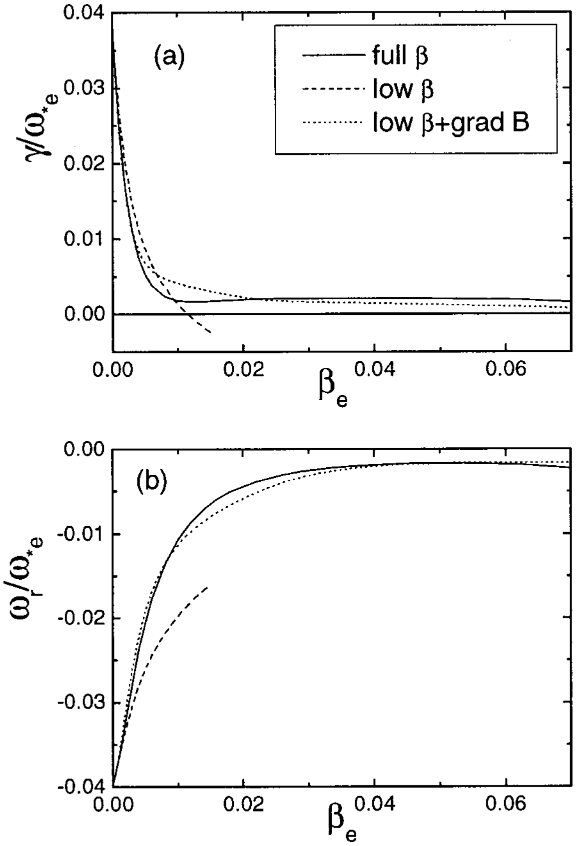

FIG. 1. Mode growth rate (a) and frequency (b) vs β_e for $\eta_i = \eta_e = 2.0$, $m_i/m_e = 1836$, $\beta_i = \beta_e$, $L_n/L_s = 0.025$, and $k_y = 1$. The solid, dashed, and dotted lines denote the results from the full β model, the low β model, and the low β model with the ∇B drift effect addition, respectively.

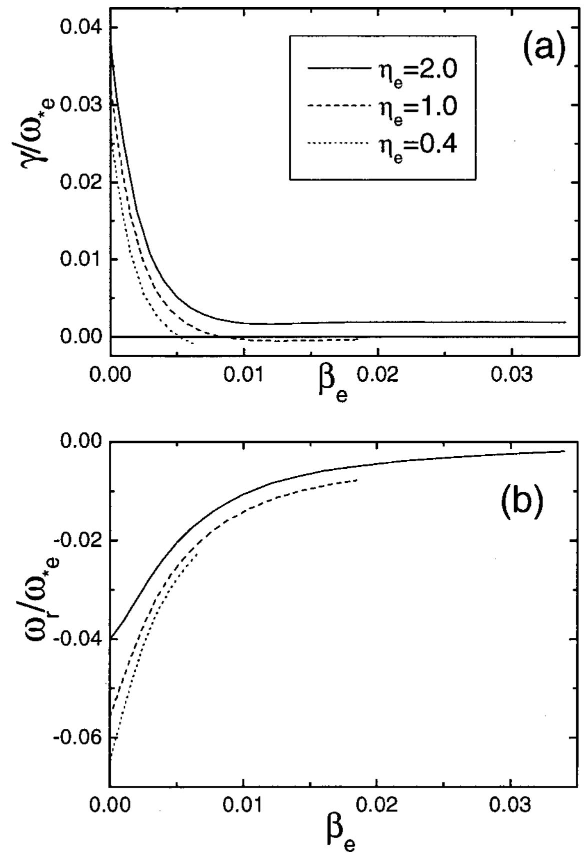

FIG. 2. The same as Fig. 1 except for $\eta_e = 2.0$, 1.0 or 0.4. All the results are from the full β model.

II. INTEGRAL EIGENMODE EQUATIONS

Consider a sheared magnetic field with a magnetic gradient

$$\vec{B} = B_0 \left[\hat{z} \left(1 + \frac{x}{L_B} \right) + \hat{y} \frac{x}{L_s} \right], \tag{1}$$

where L_s and L_B are the scale lengths of the magnetic shear and the magnetic gradient, respectively. The magnetic gradient is included to maintain the pressure equilibrium for high β plasmas in a slab, so L_B is not independent of the pressure profiles,

$$L_n/L_B = \sum_j (\beta_j/2)(1+\eta_j), \quad j = i,e. \tag{2}$$

Here, $L_n^{-1} = -(1/n_j)dn_j/dx$, $\eta_j = d \ln T_j / d \ln n_j$, and $\beta_j = 8\pi n_j T_j / B^2$.

The equilibrium distributions for ions and electrons are

$$f_{0j} = \frac{n(X_{gj})}{\pi^{3/2} v_{tj}^3} \exp\left(-\frac{v^2}{v_{tj}^2} \right), \quad v_{tj} = \sqrt{\frac{2T_j(X_{gj})}{m_j}}. \tag{3}$$

Here $X_{gj} = x - v_y/\Omega_j$ is the guiding center variable and $\Omega_j = -q_j B / m_j c$ is the gyrofrequency.

We introduce three fluctuating scalar fields: $\tilde{\phi}$, $\tilde{A}_\parallel$ $(=\tilde{A}\cdot\hat{b})$, and $\tilde{A}_2 (=(\tilde{A}\times\hat{e}_\perp)\cdot\hat{b})$, where all perturbed quantities have the form $\tilde{p}(\vec{r},t) = p(x)\exp(ik_y y - i\omega t)$,

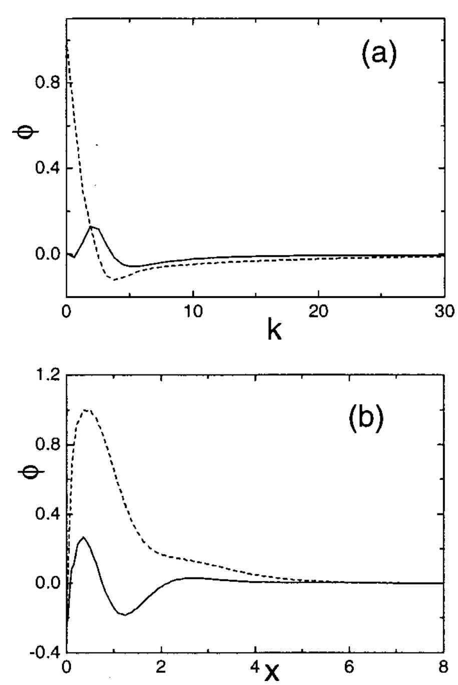

FIG. 3. Mode structure (a) $\phi(k)$ vs k and (b) $\phi(x)$ vs x for $\beta_e = \beta_i = 0$. The solid and dashed lines denote the real and imaginary parts. The other parameters are the same as for Fig. 1.

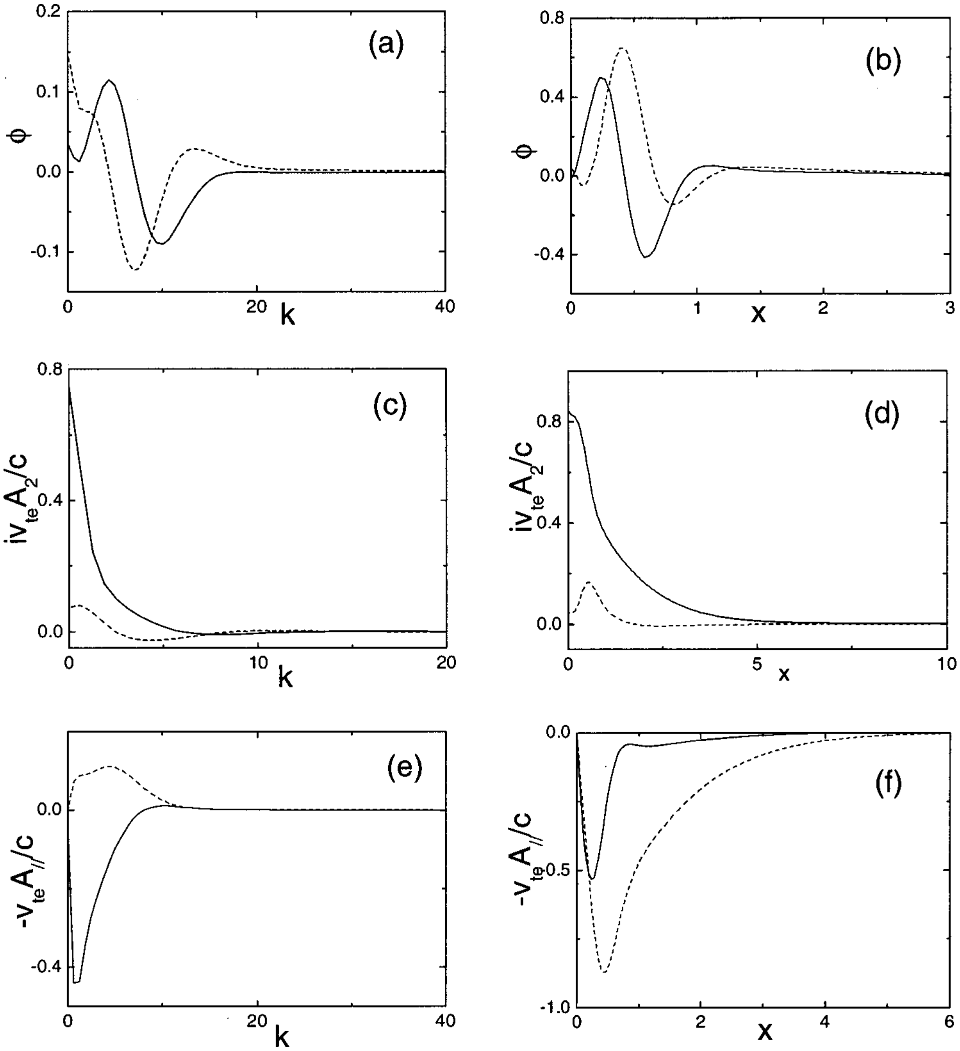

FIG. 4. Mode structure (a) $\phi(k)$ vs k; (b) $\phi(x)$ vs x; (c) $A_2(k)$ vs k; (d) $A_2(x)$ vs x; (e) $A_\parallel(k)$ vs k; (f) $A_\parallel(x)$ vs x for $\beta_e=\beta_i=0.005$. The other parameters are the same as in Fig. 1.

$\hat{e}_\perp=\vec{k}_\perp/|k_\perp|$, $\vec{k}_\perp=k_y\hat{y}-i\partial/\partial x\hat{x}$, and $\hat{b}=\vec{B}/|B|$. Assuming the fluctuations with $\omega\ll|\Omega_j|$ and $k\lambda_d\ll 1$, using the linearized Vlasov equation and integrating along unperturbed orbits give the perturbed distribution functions for the electrons and ions

$$f_{1j}=-\frac{q_jf_{0j}}{T_j}\phi(x)-i\frac{q_jf_{0j}}{T_j}\int_{-\infty}^{t}\left(\omega+\frac{k_yT_j}{\Omega_jm_j}\frac{1}{f_{0j}}\frac{\partial f_{0j}}{\partial X_{gj}}\right)\times\left[\phi'-\frac{1}{c}(\nu'_\parallel A'_\parallel+\nu'_2A'_2)\right]dt', \quad (4)$$

where $\nu'_2=(\vec{\nu}'\times\hat{e}_\perp)\cdot\hat{b}$.

Fourier transforming $p(x)=1/\sqrt{2\pi}\int p(k)\exp(ikx)dk$ gives the description equations in the k space. The quasineutrality condition gives

$$\sum_j\frac{q_j^2n_0}{T_j}\left\{\hat{\phi}(k)+\left(\frac{1}{2\pi}\right)\int dk'\int dx\exp[i(k'-k)x]\times\left[L_j(0,0,0,0)\hat{\phi}(k')+\frac{\nu_{tj}}{\nu_{te}}L_j\left(0,1,\frac{1}{2},0\right)\hat{A}_2(k')+\frac{\nu_{tj}}{\nu_{te}}L_j(0,0,0,1)\hat{A}_\parallel(k')\right]\right\}=0, \quad (5)$$

and the perpendicular and parallel components of Ampere's law are

$$\hat{A}_2(k)-\sum_j\frac{\beta_j}{2\pi b_j}\left\{\int dk'\int dx\exp[i(k'-k)x]\times\left[\frac{\nu_{te}}{\nu_{tj}}L_j\left(1,0,\frac{1}{2},0\right)\hat{\phi}(k')+L_j(1,1,1,0)\hat{A}_2(k')+L_j\left(1,0,\frac{1}{2},1\right)\hat{A}_\parallel(k')\right]\right\}=0, \quad (6)$$

$$\hat{A}_\parallel(k)-\sum_j\frac{\beta_j}{2\pi b_j}\left\{\int dk'\int dx\exp[i(k'-k)x]\times\left[\frac{\nu_{te}}{\nu_{tj}}L_j(0,0,0,1)\hat{\phi}(k')+L_j\left(0,1,\frac{1}{2},1\right)\hat{A}_2(k')+L_j(0,0,0,2)\hat{A}_\parallel(k')\right]\right\}=0. \quad (7)$$

Here

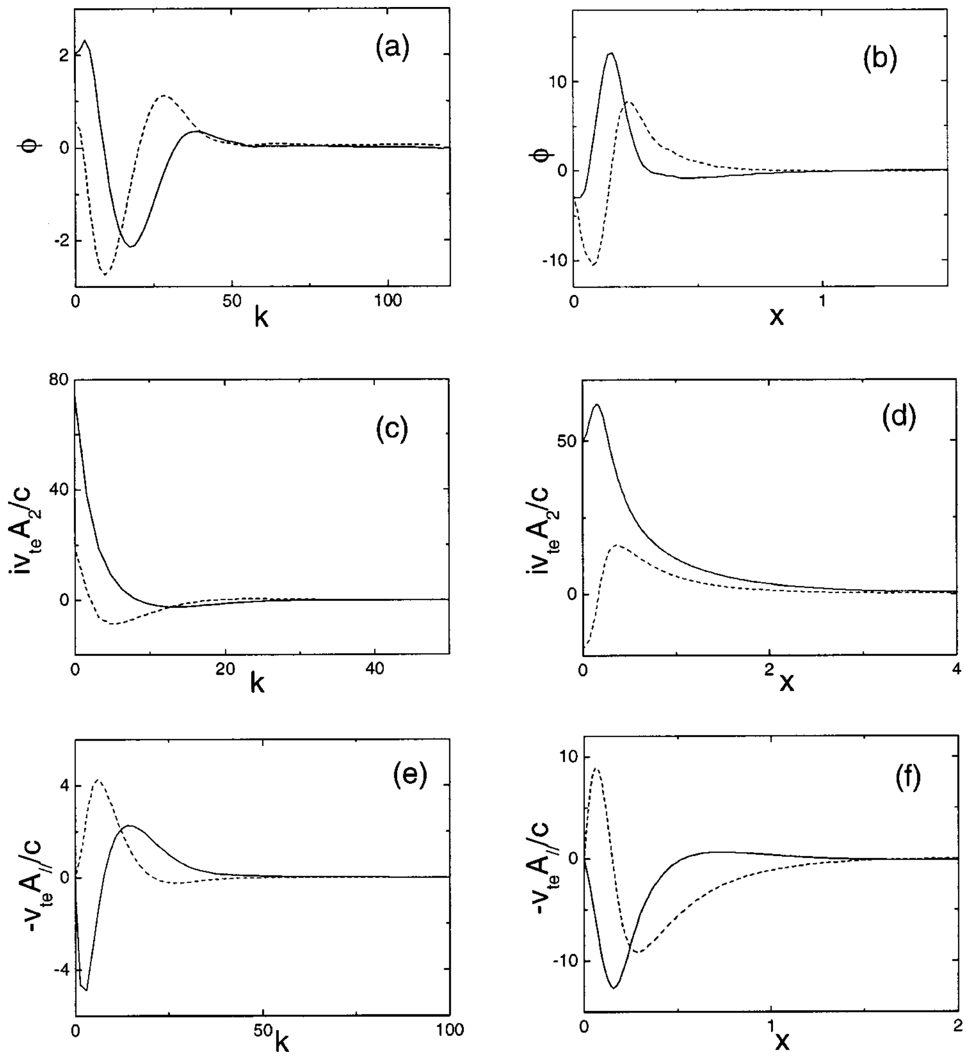

FIG. 5. The same as in Fig. 4 except for $\beta_e=\beta_i=0.05$.

$$L_j(m,n,s,l)=\left(\frac{-q_j}{|q_j|}\right)^{m+n}\int_0^{+\infty}dt\, t^s \exp(-t)\times J_m(\sqrt{2b_jt})J_n(\sqrt{2b_j't})\frac{\omega_{*j}}{\omega-\omega_{Dj}t}K_{lj}, \tag{8}$$

$$K_{0j}=\left(\frac{\omega}{\omega_{*j}}-1\right)[\xi_jZ(\xi_j)]-\eta\left[\xi_j^2+\left(\xi_j^2-\frac{1}{2}\right)\xi_jZ(\xi_j)\right]-\eta(t-1)[\xi_jZ(\xi_j)], \tag{9}$$

$$K_{1j}=\frac{k_\parallel}{|k_\parallel|}\xi_j\left[K_{0j}+\left(\frac{\omega_0}{\omega_{*j}}-1\right)-\eta(t-1)\right], \tag{10}$$

$$K_{2j}=\frac{k_\parallel}{|k_\parallel|}\xi_jK_{1j}, \tag{11}$$

$$\omega_{*j}=(k_yT_j)/(\Omega_jm_jL_n),\quad \omega_{Dj}=-\omega_{*j}L_n/L_B,$$
$$b_j=k_\perp^2\rho_j^2/2,\quad b_j'=k_\perp'^2\rho_j^2/2,\quad \rho_j=\nu_{tj}/\Omega_j,$$
$$\xi_j=(\omega-\omega_{dj}t)/|k_\parallel|\nu_{tj},\quad k_\parallel=(x/L_s)k_y,$$
$$k_\perp^2=k_y^2+k^2,\quad k_\perp'^2=k_y^2+k'^2,\quad \hat{\phi}=\phi,$$
$$\hat{A}_2=i\nu_{te}A_2/c,\quad \hat{A}_\parallel=-\nu_{te}A_\parallel/c,$$

and $Z(\xi)$ is the plasma dispersion function. Equations (5)–(7) are the basic equations that govern the behavior of the modes. This model is valid for all orders of β, so we call it the full β model. Omitting the coupling to the compressional Alfvén waves (CAWs) and the magnetic gradient effects, that is, $\hat{A}_2=0$ and $L_B\to\infty$, gives the same equations as Eqs. (4) and (5) in Dong *et al.*,[8] which is valid in low β assumption so is called the low β model. In addition, the local treatment ($k=k'=0, k_\parallel=$const) simplifies Eqs. (5)–(7) to the local dispersion equations in Gao *et al.*[16]

III. NUMERICAL RESULTS

The integral equations, Eqs. (5)–(7), are solved using the Raleigh–Ritz technique.[19] The detailed procedure is well documented in Dong *et al.*[20] and will only be outlined here.

The fluctuating field can be expanded in terms of rectangular functions,

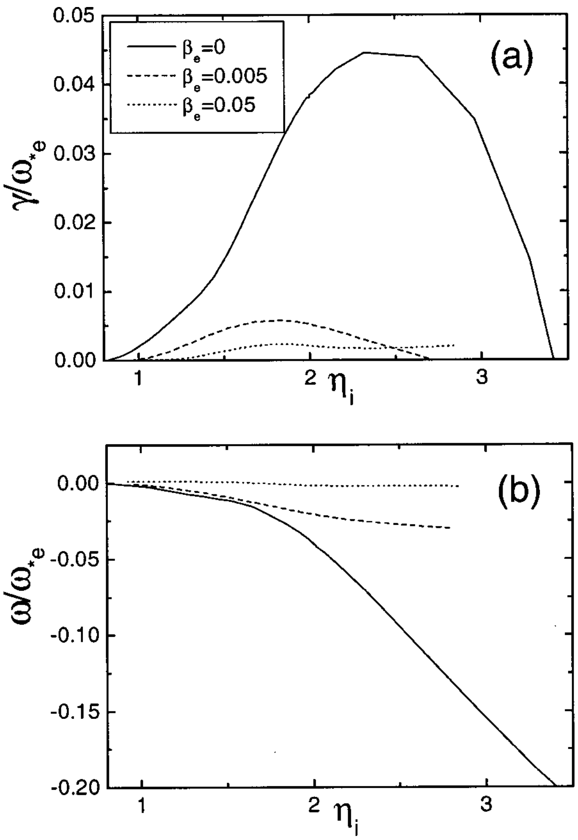

FIG. 6. Mode growth rate (a) and frequency (b) vs η_i for $\beta_e=\beta_i=0$, 0.005 and 0.05. The other parameters are the same as in Fig. 1.

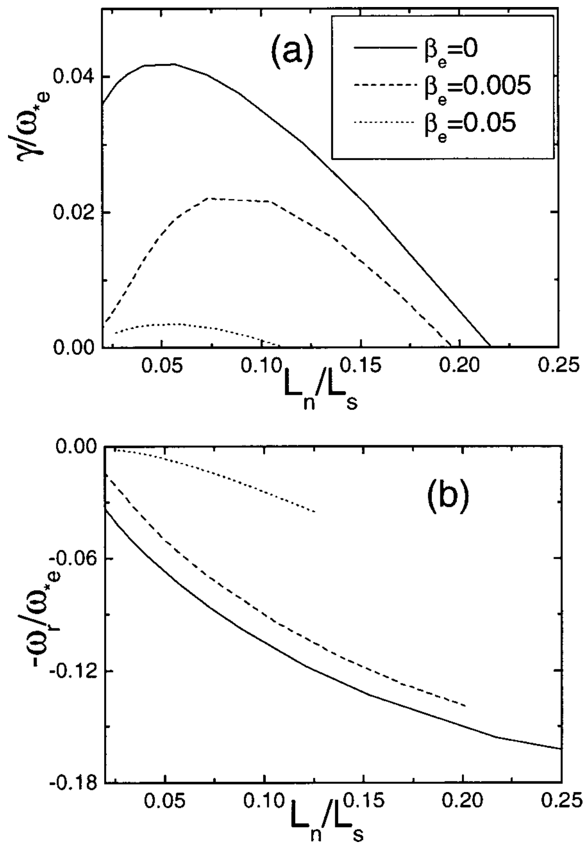

FIG. 8. Mode growth rate (a) and frequency (b) vs L_n/L_s for $\beta_e=\beta_i=0$, 0.005, and 0.05. The other parameters are the same as in Fig. 1.

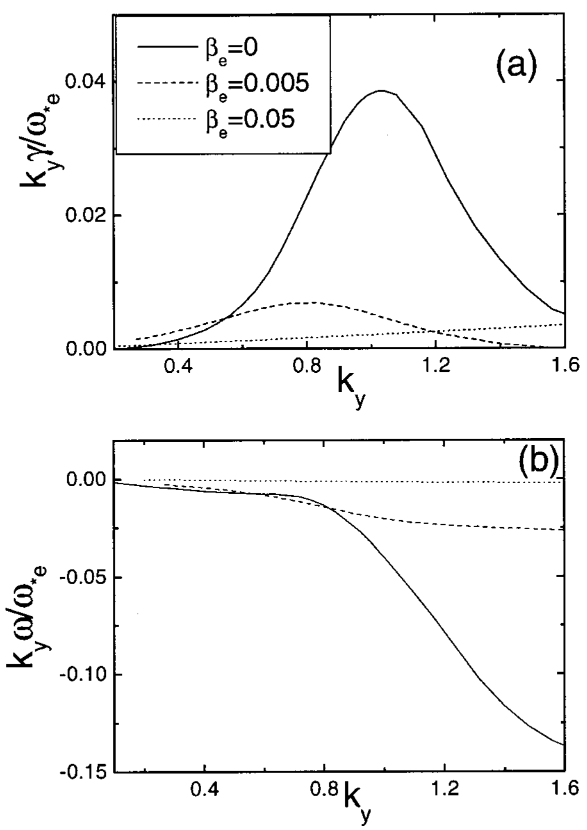

FIG. 7. Mode growth rate (a) and frequency (b) vs k_y for $\beta_e=\beta_i=0$, 0.005, and 0.05. The other parameters are the same as in Fig. 1.

$$\hat{p}^s(k)=\sum_{j=1}^{N} a_j^s\chi_j(k), \quad \chi_j(k)=\begin{cases}1, & k\in[(j-1)h,jh),\\ 0, & k\notin[(j-1)h,jh),\end{cases} \tag{12}$$

where $\hat{p}^1$, $\hat{p}^2$, and $\hat{p}^3$ denote $\hat{\phi}$, $\hat{A}_2$, and $\hat{A}_\parallel$, respectively. Substituting into Eqs. (5)–(7), multiplying the resulting equations by $\chi_i(k)$ and integrating over k, we obtain a set of linear algebraic equations

$$M_{ij}^1 a_j^1+P_{ij}^1 a_j^2+Q_{ij}^1 a_j^3=0, \tag{5$'$}$$

$$M_{ij}^2 a_j^1+P_{ij}^2 a_j^2+\Omega_{ij}^2 a_j^3=0, \tag{6$'$}$$

$$M_{ij}^3 a_j^1+P_{ij}^3 a_j^2+Q_{ij}^3 a_j^3=0. \tag{7$'$}$$

The full coefficient matrix is then

$$K=\begin{pmatrix} M^1 & P^1 & Q^1\\ M^2 & P^2 & Q^2\\ M^3 & P^3 & Q^3\end{pmatrix}. \tag{13}$$

The eigenfrequency ω is given by the relation

$$\lambda=0,$$

where λ is the minimal non-negative eigenvalue of K. The corresponding mode structure can also be obtained. A notable problem is the integral in the perpendicular velocity space, Eq. (8). Since the plasma dispersion function Z is not independent of t, the integral should be accurate enough to describe the resonant regime.

The parameters chosen here are the same as the usual Linsker's parameters:[4,8,15] $\eta_e=2$, $\eta_i=2$, $T_e/T_i=1$, $m_i/m_e=1836$, $L_n/L_s=0.025$, and $k_y=1$ unless otherwise stated. For convenience, all the lengths have been normalized to $|\rho_i|$ in the following. In addition, all the results that are not otherwise stated are obtained from the full β model.

Shown in Fig. 1 is the mode growth rate and frequency as functions of β_e (or $\beta/2$). The mode cannot be stabilized by finite β when the ∇B effect is included in the model (the solid and the dotted lines). However, the dashed lines show that the mode is stabilized at $\beta_e\approx 1.4\%$ if the ∇B effect is not considered. This is completely consistent with the previous result.[8] It is also noted that in the low β regime, increasing β reduces the frequency and the growth rate more rapidly in the models with ∇B than in the model without ∇B. Consequently, the frequency reaches a very low level very soon and is not changed efficiently by β any longer. These effects are explained in the next paragraph using the analysis of a simplified model.

Local study[16] shows that the inverse Landau damping dominates the stability property of the mode. That is, β affects the growth rate mainly by changing the mode frequency. With the fluid approximation ($\nu_{ti}<|\omega/k_\parallel|<\nu_{te}$), the mode frequency is governed by Eq. (8) in Gao *et al.*,[16] which is rewritten here without the small term $i\delta_i$,

$$\left[1+\frac{\omega_{*e}}{\omega}(\eta_i b_i-1)\right]\left[1-\frac{\beta_i}{b_i}\frac{\omega^2}{k_\parallel^2\nu_{ti}^2}\frac{1}{\tau}\left(1-\frac{\omega_{*e}}{\omega}\right)\right] +\frac{\beta_i}{b_i}\frac{\omega^2}{k_\parallel^2\nu_{ti}^2}\frac{1}{\tau}\left(1-\frac{\omega_{*e}}{\omega}\right)^2=0. \quad (14)$$

Then

$$\frac{\partial(\omega/\omega_{*e})}{\partial\beta}=\frac{-\eta_i(\omega/\omega_{*e}-1)}{\beta_i\eta_i+\tau(\eta_i b_i-1)k_\parallel^2\nu_{ti}^2/\omega^2}. \quad (15)$$

As $\omega/\omega_{*e}<0$ and $\eta_i b_i>1, \partial(\omega/\omega_{*_e})/\partial\beta$ is positive and $|\partial(\omega/\omega_{*_e})/\partial\beta|$ decreases with increasing β and decreasing $|\omega|$. The decrease of $|\omega|$ reduces the inverse Landau damping, so that the growth rate γ decreases. Both the mode frequency and the growth rate will flatten gradually as β increases, as has been verified by previous numerical results.[8,15,16] Merely, with the usual parameters, the mode has already been stable before the frequency flattens too much. However, consideration of the ∇B effect makes the problem more complicated since ∇B obviously reduces the mode frequency. In the low β regime this reduction reduces the growth rate, while the reduction makes the frequency so low that β cannot affect the frequency efficiently in the high β regime. Figure 2 shows how sensitively the frequency affects the stability property. As η_e decreases, the frequency increases and the growth rate decreases. When η_e is less than 1, the mode has been stabilized before the frequency and the growth rate flatten though the full β model is used.

On the other hand, the unstable modes are those with $\omega\sim O(k_\parallel\nu_{ti})$ because of the inverse Landau damping. But then, $k_\parallel$ is artificially chosen in the local model. In the nonlocal model $k_\parallel=(x/L_s)k_y$, so those modes with very low frequencies can be unstable in the small x region. The numerical results in Figs. 3, 4, and 5 verify this point through the mode structure in k space and x space at $\beta=0$, 0.01, and 0.1, respectively. A mode at high β is localized at a much smaller length scale in x space than a mode at low β. Moreover, the mode length scale in k space increases with β, which implies that the differential approach is not appropriate to deal with the problem in high β cases.

Figure 6 shows the mode frequency and the growth rate as functions of η_i for $\beta=0$, 0.01, and 0.1. The mode is destabilized not only at low β but also at high β when η_i exceeds a finite value, which indicates the mode is driven by finite η_i even though the η_i dependence is weakened as β increases. Moreover, the upper η_i stability regime (i.e., $\gamma<0$ as $\eta_i>\eta_{\rm up}$) exists in the low β regime but is not found in the high β regime.

The k_y spectra for different β are presented in Fig. 7. Similar with the η_i dependence, the effect of k_y is weakened as β increases. This trend was also shown in previous results[8] using the low β model.

In addition, the magnetic shear can stabilize the mode even in the high β regime. Figure 8 shows the mode frequency and growth rate as functions of L_n/L_s for $\beta=0$, 0.01, and 0.1. Since the mode frequency increases with the L_n/L_s, the high β mode is stable at high L_n/L_s.

IV. CONCLUSIONS AND DISCUSSION

A series of integral equations is developed to study the slab drift instabilities in any β plasmas. Both components of the perturbed vector potential, $\tilde{A}_\parallel$ and $\tilde{A}_2$, are considered in the equations, as well as the perturbed electrostatic potential $\tilde{\phi}$. The magnetic gradient effect is included to keep pressure balance. The ITG modes are studied and found hardly stabilized by finite β with the magnetic gradient effect inclusion. The stability property of the high β mode is sensitive to the mode frequency. Generally speaking, the lower frequency modes are more difficult to be stabilized since β cannot effectively change the frequency in the low frequency regime. On the other hand, the magnetic shear can stabilize the high β mode.

The present study was performed in the slab geometry. The two important events are the flattening of the frequency in the high β regime and the reducing of the frequency due to the magnetic gradient. However, previous toroidal results[11] in the low β limit did not reveal the picture of frequency flattening with β. That is, the analyses and results in this work may not be appropriate for the toroidal system. However, a general idea may be useful in the toroidal work. A favorable factor in a simplified analysis (or in some special conditions) may become an unfavorable factor in a complete analysis (or in other conditions). For example, the magnetic gradient enhances the finite β stabilization effects on the local mode and the nonlocal mode in the high frequency regime while results in the fact that the nonlocal mode cannot be stabilized in the low frequency regime.

The k_y spectrum shows that the high β ITG mode spreads in a very wide k_y region. If the wavelength is so short that $k_y\rho_e\sim 1$, the electron temperature gradient driven mode[21] (ETG mode) may dominate. Although the ETG mode has a small perpendicular wavelength, its growth rate is found to greatly exceed the observed $E\times B$ shearing rate.[22] The full kinetics of the electrons is taken into account in the integral equations presented in this work. Therefore, the equations can be used to study the slab ETG mode without any modification.

ACKNOWLEDGMENTS

This work was supported by the National Science Foundation of China, Grants No. 19889506 and No. 19875014.

[1] B. Coppi, M. N. Rosenbluth, and R. Z. Sagdeev, Phys. Fluids **10**, 582 (1967).
[2] M. Greenwald, D. Gwinn, S. Milora, J. Parker, R. Parker, S. Wolfe, M. Besen, F. Camacho, S. Fairfax, C. Fiore, M. Foord, R. Gandy, C. Gomez, R. Granetz, B. La Bombard, B. Lipschultz, B. Lloyd, E. Marmar, S. McCool, D. Pappas, R. Petrasso, P. Pribyl, J. Rice, D. Schuresko, Y. Takase, J. Terry, and R. Watterson, Phys. Rev. Lett. **53**, 352 (1984).
[3] S. D. Scott, P. H. Diamond, R. J. Fonck, R. B. Howell, K. P. Jahnig, G. Schilling, E. J. Synakowski, M. C. Zarnstorff, C. E. Bush, E. Fredrickson, K. W. Hill, A. C. Janos, D. K. Mansfiled, D. K. Owens, H. Park, G. Pautasso, A. T. Ramsey, J. Schivell, G. D. Tait, W. M. Tang, and G. Taylor, Phys. Rev. Lett. **64**, 531 (1990).
[4] R. Linsker, Phys. Fluids **24**, 1485 (1981).
[5] T. S. Hahm and W. M. Tang, Phys. Fluids B **1**, 1185 (1989).
[6] F. Romanelli, Phys. Fluids B **1**, 1018 (1989).
[7] J. Q. Dong, W. Horton, and J. Y. Kim, Phys. Fluids B **4**, 1867 (1992).
[8] J. Q. Dong, P. N. Guzdar, and Y. C. Lee, Phys. Fluids **30**, 2694 (1987).
[9] Y.-K. Pu and S. Migliuolo, Phys. Fluids **28**, 1722 (1985).
[10] W. Horton, J. E. Sedlak, D.-I. Choi, and B. G. Hong, Phys. Fluids **28**, 3050 (1985).
[11] J. Y. Kim, W. Horton, and J. Q. Dong, Phys. Fluids B **5**, 4030 (1993).
[12] A. Jarmen, P. Anderson, and J. Weiland, Nucl. Fusion **27**, 941 (1987).
[13] J. Weiland and A. Hirose, Nucl. Fusion **32**, 151 (1992).
[14] B. G. Hong, W. Horton, and D. I. Choi, Plasma Phys. Controlled Fusion **31**, 1291 (1989).
[15] J. V. M. Reynders, Phys. Plasmas **1**, 1953 (1994).
[16] Zhe Gao, J. Q. Dong, G. J. Liu, and C. T. Ying, Phys. Plasmas **8**, 2816 (2001).
[17] A. Sykes and the START, NBI, MAST and Theory Teams, Nucl. Fusion **39**, 1271 (1999).
[18] W. M. Tang, G. Rewoldt, and E. A. Frieman, Phys. Fluids **23**, 2454 (1980).
[19] L. M. Delves and J. Walsh, *Numerical Solution of Integral Equations* (Clarendon, Oxford, 1974).
[20] J. Q. Dong, P. N. Guzdar, and Y. C. Lee, Phys. Fluids **30**, 399 (1987).
[21] Y. C. Lee, J. Q. Dong, P. N. Guzdar, and C. S. Liu, Phys. Fluids **30**, 1331 (1987).
[22] B. W. Stallard, C. M. Greenfield, G. M. Staebler, C. L. Rettig, M. S. Chu, M. E. Austin, D. R. Baker, L. R. Baylor, K. H. Burrell, J. C. DeBoo, J. S. deGrassie, E. J. Doyle, J. Lohr, G. R. McKee, R. L. Miller, W. A. Peebles, C. C. Petty, R. I. Pinsker, B. W. Rice, T. L. Rhodes, R. E. Waltz, and L. Zeng, Phys. Plasmas **6**, 1978 (1999).